Combined QM/MM MD Study of $HCOO^-$−Water Hydrogen Bonds in Aqueous Solution

Apirak Payaka,[†] Anan Tongraar,*[,†] and Bernd Michael Rode[‡]

School of Chemistry, Institute of Science, Suranaree University of Technology, Nakhon Ratchasima 30000, Thailand, and Department of Theoretical Chemistry, Institute of General, Inorganic and Theoretical Chemistry, University of Innsbruck, Innrain 52a, A-6020 Innsbruck, Austria

Received: November 25, 2008; Revised Manuscript Received: February 22, 2009

Characteristics of $HCOO^-$−water hydrogen bonds in dilute aqueous solution have been investigated by means of combined HF/MM and B3LYP/MM molecular dynamics simulations, in which the central $HCOO^-$ and its surrounding water molecules were treated at HF and B3LYP levels of accuracy, respectively, using DZV+ basis set. Both HF/MM and B3LYP/MM simulations supply information that the hydrogen bonds between $HCOO^-$ oxygens and first-shell waters are relatively strong, that is, compared to the water−water hydrogen bonds. Regarding to the HF/MM and B3LYP/MM trajectories, it is observed that first-shell waters are either "loosely" or "tightly" bound to their respective $HCOO^-$ oxygen atoms, showing large fluctuations in the hydration number, varying from 2 to 6 (HF/MM) and 1 to 5 (B3LYP/MM), with the prevalent value of 3. Comparing the HF and B3LYP methods for the description of QM treated region, the first one leads to slightly too weak and thus longer hydrogen bonds, while the latter predicts them stronger but with the wrong dynamical data.

1. Introduction

Investigations of the microstructure and dynamics of ions solvated in aqueous electrolyte solutions have long been a scientific interest because of their diverse functions in many chemical and biological processes.[1−3] In experiments, several techniques such as X-ray (XD) and neutron diffraction (ND), as well as nuclear magnetic resonance (NMR), infrared absorption, X-ray absorption fine structure (EXAFS), and X-ray absorption near edge structure (XANES) spectroscopy have been used to obtain detailed knowledge of ions in aqueous solution.[4−6] However, most of these experimental techniques require major resources of laboratory equipment, but even then the results often show large discrepancies, especially for very dilute solution, due to technical limitations.[7,8]

Alternatively, computer simulations by means of Monte Carlo (MC) or molecular dynamics (MD) have become a powerful tool to study such solutions. For more than three decades, a large number of MC and MD simulations have been carried out, providing microscopic details for numerous solvated ions.[9−13] Because most of the earlier works had to rely on classical molecular mechanical force fields for describing all kinds of interactions, the simulation results, in particular, the hydration structure, as well as the dynamics of solvent molecules surrounding the ions, crucially depended on the quality and completeness of the potential functions employed in the simulations.[14−16] To accurately describe the properties of ions in aqueous solution, it has been demonstrated that "quantum effects" are significant and that inclusion of these effects in the simulations is mandatory.[17] Since the performance of ab initio quantum mechanical calculations for a condensed-phase system consisting of a large number of molecules is still beyond the current computational feasibility, the Car−Parrinello molecular dynamics (CPMD) method[18,19] reduced the computational expense by using a simple density functional and a moderate system size containing about 30−60 solvent molecules. Albeit the CPMD technique has meanwhile been well-established for the study of solvated ions,[20−23] the simplification of the quantum mechanics employed has led to some severe limitations in accuracy of this scheme for the treatment of electrolyte solutions.[17]

With regard to the limits in computing power, another approach is to apply a hybrid quantum mechanics/molecular mechanics (QM/MM) method.[24−27] By the QM/MM technique, the chemically most relevant region, that is, a sphere including the ion and its surrounding solvent molecules, is described as accurately as needed using quantum mechanics (QM), whereas the rest of the system is handled by molecular mechanics (MM) with appropriate force fields. In the course of QM/MM scheme, the complicated many-body contributions as well as the polarization effects, which are hardly accessible through the basic assumptions underlying the classical models, can be reliably included into the specified region. In recent years, a number of QM/MM MD simulations have been carried out for various ions in solutions, providing many new insights into the solvation structure and dynamics of the solvated ions.[28−35]

In the present study, the behavior of formate ion ($HCOO^-$), the simplest species containing the carboxylate (COO^-) functional group, solvated in water was of interest. According to NMR experiments with carboxylic acids, it has been suggested that each carboxylate group is surrounded by 5.0−6.5 water molecules.[36] For $HCOO^-$, the results obtained from X-ray and neutron scattering of aqueous NaHCOO[37] and KHCOO[38] solutions as well as from infrared measurements of a series of KHCOO concentrations[38]have inferred that the hydration number per $HCOO^-$ oxygen atom is below 2.5. In terms of theoretical investigations, early MC simulations with "optimized potentials for liquid simulations" (OPLS) empirical force fields have been performed, revealing strong pronounced pair correlation functions between each $HCOO^-$ oxygen and the oxygen/hydrogen atoms of water molecules, with a hydration

* Corresponding author. E-mail: anan_tongraar@yahoo.com. Fax: 0066-44-224017.
[†] Suranaree University of Technology.
[‡] University of Innsbruck.

10.1021/jp810341u CCC: $40.75
Published on Web 03/06/2009

number of 3.6.[39] Recently, CPMD simulations of aqueous $HCOO^-$ have been carried out,[40] showing structural features significantly different from those predicted by the OPLS potentials. According to the CPMD simulation using the BLYP functional, a hydration number of 2.45 per $HCOO^-$ oxygen was predicted, which is in good accord with recent experiments.[37,38] However, the use of another exchange correlation functional, namely, PW91, led to hydration numbers ranging from 2.12 to 2.66. With regard to the CPMD method, it should be taken into account that the system's size under investigation was rather small, consisting of only 53 water molecules, and that only the simple GGA density functionals were employed. In this work, it was of particular interest, therefore, to apply the QM/MM technique in order to obtain a description of the $HCOO^-$-water coordination in aqueous solution based on noncorrelated ab initio quantum mechanics and at DFT level using a more accurate hybrid functional.

2. Methods

According to the QM/MM MD technique,[17,28−35] the system is partitioned into two parts, namely, QM and MM regions. The total interaction energy of the system is defined as

$$E_{\text{total}} = \langle \Psi_{\text{QM}} | \hat{H} | \Psi_{\text{QM}} \rangle + E_{\text{MM}} + E_{\text{QM-MM}} \qquad (1)$$

where $\langle \Psi_{\text{QM}} | \hat{H} | \Psi_{\text{QM}} \rangle$ refers to the interactions within the QM region, while E_{MM} and $E_{\text{QM-MM}}$ represent the interactions within the MM and between the QM and MM regions, respectively. The QM region, the most interesting subsystem, which includes $HCOO^-$ and its nearest-neighbor water molecules, is treated quantum mechanically, while the rest of the system is described by classical pair potentials. Considering the exchange of water molecules between the QM and MM regions, which can occur frequently during the QM/MM simulations, the forces acting on each particle in the system are switched according to which region the water molecule is entering or leaving and can be defined as

$$F_i = S_{\text{m}}(r) F_{\text{QM}} + (1 - S_{\text{m}}(r)) F_{\text{MM}} \qquad (2)$$

where F_{QM} and F_{MM} are quantum mechanical and molecular mechanical forces, respectively. $S_{\text{m}}(r)$ is a smoothing function[41]

$$\begin{aligned} S_{\text{m}}(r) &= 1, \quad \text{for } r \le r_1 \\ S_{\text{m}}(r) &= \frac{(r_0^2 - r^2)^2 (r_0^2 + 2r^2 - 3r_1^2)}{(r_0^2 - r_1^2)^3}, \quad \text{for } r_1 < r \le r_0 \\ S_{\text{m}}(r) &= 0, \quad \text{for } r > r_0 \end{aligned} \qquad (3)$$

where r_1 and r_0 are distances characterizing the start and the end of the smoothing region, for which an interval of 0.2 Å has been found to be optimal to ensure a continuous change of forces at the boundary between QM and MM regions.

In the QM/MM technique, the quality of the simulation results crucially depends on the selection of QM method, basis set, and QM size. Because the performance of QM/MM MD simulations in conjunction with correlated ab initio methods is still far too time-consuming, the HF and the hybrid density functional B3LYP methods were the only possible alternatives for the present study. To simply check whether the HF and B3LYP methods are adequate for this particular system,

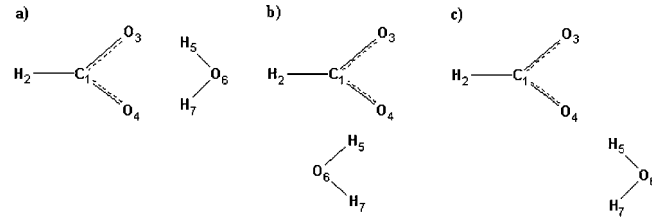

Figure 1. (a) Cyclic, (b) anti, and (c) syn $HCOO^-$−H_2O complexes.

geometry optimizations of cyclic, anti, and syn $HCOO^-$−H_2O clusters (see Figure 1) were carried out at HF, B3LYP, MP2, and CCSD levels of accuracy using DZV+[42] and aug-cc-pvdz[43−45] basis sets. As can be seen from the optimized parameters in Table 1, the B3LYP hydrogen-bond lengths and energies are close to those of the correlated ab initio methods using the larger basis set, while the HF results show good agreement with the correlated data when the smaller basis set, DZV+, is employed. Overall, the H-bond length and energy ordering of the three clusters predicted by the HF and B3LYP methods are in accord with the correlated results. This suggests that quantum mechanical calculations by both HF and B3LYP methods would be reliable enough to achieve a sufficient level of accuracy in the QM/MM simulations. The quality of the HF method has been well demonstrated in previous QM/MM studies,[17,28−35] even for the treatment of anions, implying that the effects of electron correlation are small enough to be neglected.[30,31] In a recent QM/MM MD simulation of pure water,[46] it has been shown that the HF method with a sufficiently large QM size could provide detailed information of pure water in good agreement with the MP2-based simulation and with experimental data concerning hydrogen-bond structure and lifetime. The B3LYP method, although inferior for most hydrated cations,[17,34] was also employed in the present work because it has been claimed that this method could predict reasonable data for weakly bound H-bonded systems.[35,47]

Because a satisfactory description of anions usually requires diffuse basis functions, the DZV+ basis set[42] was chosen, considered as a suitable compromise between the quality of the simulation results and the requirement of CPU time. To define the size of the QM region, preliminary HF/MM and B3LYP/MM simulations in which only the $HCOO^-$ ion was treated quantum mechanically using HF and B3LYP methods, while the rest of the system was described by classical pair potentials, were performed. In the resulting C−O_w radial distribution functions (RDFs) (data not shown), both HF/MM and B3LYP/MM simulations showed first C−O_w minima at around 5.0 Å, and integrations up to this C−O_w distance yielded about 18−20 water molecules. This implied that a QM size with a radius of 5.0 Å seemed to be desirable for the present study. However, the evaluation of QM forces for all particles within this QM size is still beyond the limit of our computational facility. Therefore, a smaller QM size with radius of 4.0 Å was chosen (i.e., the values of r_1 and r_0 in eq 3 were set with respect to the C---O_w distances to 3.8 and 4.0 Å, respectively), which contains the central $HCOO^-$ and about 12−14 nearest-neighbor water molecules.

A flexible model, which describes intermolecular[48] and intramolecular[49] interactions, was employed for water. This flexible water model allows explicit hydrogen movements, thus ensuring a smooth transition when water molecules move from the QM region with its full flexibility to the MM region. The pair potential functions for describing $HCOO^-$−H_2O interactions were newly constructed. The 6015 HF and 5966 B3LYP

TABLE 1: Stabilization Energies and some Selected Structural Parameters of the Optimized Cyclic, Anti, and Syn $HCOO^-$−H_2O complexes[a]

method	HF	B3LYP	MP2	CCSD
		Cyclic Complex		
ΔE (kcal·mol^{-1})	−20.17 (−16.31)	−22.09 (−18.09)	−21.33 (−19.22)	−21.16 (−18.80)
R_{1-2} (Å)	1.1008 (1.1176)	1.1218 (1.1318)	1.1233 (1.1282)	1.1262 (1.1301)
R_{1-3}, R_{1-4} (Å)	1.2665 (1.2370)	1.2913 (1.2602)	1.3121 (1.2715)	1.3047 (1.2645)
R_{3-5}, R_{4-7} (Å)	2.1372 (2.1326)	2.0211 (2.0060)	2.0977 (1.9955)	2.1115 (2.0624)
R_{5-6}, R_{6-7} (Å)	0.9592 (0.9514)	0.9911 (0.9786)	0.9915 (0.9799)	0.9892 (0.9755)
A_{3-1-4} (deg)	128.12 (129.36)	128.16 (129.27)	128.18 (129.22)	128.18 (129.33)
A_{3-5-6}, A_{4-7-6} (deg)	137.87 (141.38)	140.74 (143.70)	140.25 (144.63)	139.84 (143.87)
A_{5-6-7} (deg)	104.71 (98.67)	101.11 (96.20)	102.01 (95.31)	102.33 (96.07)
		Anti Complex		
ΔE (kcal.mol^{-1})	−18.278 (−14.13)	−20.38 (−16.42)	−18.78 (−16.75)	−18.52 (−16.25)
R_{1-2} (Å)	1.1034 (1.1185)	1.1236 (1.1315)	1.1258 (1.1286)	1.1289 (1.1306)
R_{1-3} (Å)	1.2544 (1.2274)	1.2756 (1.2482)	1.2981 (1.259)	1.2902 (1.2525)
R_{1-4} (Å)	1.2726 (1.244)	1.3004 (1.2703)	1.3189 (1.2808)	1.3125 (1.2740)
R_{4-5} (Å)	1.7066 (1.7871)	1.5815 (1.6503)	1.6844 (1.6596)	1.7081 (1.6912)
R_{5-6} (Å)	0.9782 (0.9666)	1.0284 (1.0087)	1.0166 (1.0075)	1.0094 (0.9983)
R_{6-7} (Å)	0.9506 (0.9420)	0.9770 (0.9631)	0.9796 (0.9644)	0.9799 (0.9630)
A_{3-1-4} (deg)	128.87 (129.42)	128.25 (128.82)	128.42 (128.91)	128.60 (129.09)
A_{5-6-7} (deg)	109.37 (103.41)	108.19 (102.71)	108.17 (101.95)	107.75 (102.16)
		Syn Complex		
ΔE (kcal.mol^{-1})	−17.88 (−13.44)	−19.36 (−14.70)	−17.36 (−15.38)	−18.14 (−15.00)
R_{1-2} (Å)	1.1086 (1.1174)	1.1259 (1.1247)	1.1279 (1.1371)	1.1294 (1.1235)
R_{1-3} (Å)	1.2413 (1.2313)	1.2784 (1.2539)	1.3034 (1.2620)	1.2905 (1.2463)
R_{1-4} (Å)	1.2490 (1.2220)	1.3002 (1.2673)	1.3192 (1.2836)	1.3123 (1.2677)
R_{4-5} (Å)	1.7483 (1.8068)	1.7044 (1.7685)	1.8397 (1.7523)	1.7663 (1.7611)
R_{5-6} (Å)	0.9682 (0.9527)	1.0125 (0.9907)	1.0009 (0.9938)	1.0034 (0.9668)
R_{6-7} (Å)	0.9477 (0.9426)	0.9777 (0.9624)	0.9823 (0.9665)	0.9789 (0.9605)
A_{3-1-4} (deg)	129.45 (129.91)	129.27 (129.85)	129.07 (130.15)	129.22 (129.61)
A_{5-6-7} (deg)	108.27 (102.51)	106.41 (102.31)	105.60 (101.84)	106.48 (101.08)

[a] Calculated at HF, B3LYP, MP2, and CCSD methods using DZV+ and aug-cc-pvdz (data in parentheses) basis sets.

interaction energy points for various $HCOO^-$−H_2O configurations, obtained from Gaussian98[50] calculations using aug-cc-pvdz basis set,[43−45] were fitted to the analytical forms of

$$\Delta E^{HF}_{HCOO^-\text{--}H_2O} = \sum_{i=1}^{4}\sum_{j=1}^{3}\left[\frac{A_{ij}}{r_{ij}^{4}} + \frac{B_{ij}}{r_{ij}^{8}} + C_{ij}\exp(-D_{ij}r_{ij}) + \frac{q_iq_j}{r_{ij}}\right] \quad (4)$$

and

$$\Delta E^{B3LYP}_{HCOO^-\text{--}H_2O} = \sum_{i=1}^{4}\sum_{j=1}^{3}\left[\frac{A_{ij}}{r_{ij}^{4}} + \frac{B_{ij}}{r_{ij}^{5}} + C_{ij}\exp(-D_{ij}r_{ij}) + \frac{q_iq_j}{r_{ij}}\right] \quad (5)$$

where A, B, C, and D are fitting parameters, r_{ij} denotes the distances between the ith atoms of $HCOO^-$ and the jth atoms of the water molecule and q are atomic net charges. In the present study, the charges on C, O, and H of $HCOO^-$ were obtained from Natural Bond Orbital (NBO) analysis[51−53] of the corresponding HF and B3LYP calculations, as 0.8635, −0.9201, and −0.0234 (HF) and 0.6583, −0.8197 and −0.0190 (B3LYP), respectively. The charges on O and H of water molecule were adopted from the BJH-CF2 water model[46] as −0.6598 and 0.3299, respectively. The optimized parameters for the intermolecular potentials (4) and (5) are listed in Table 2.

All simulations were performed in a canonical ensemble at 298 K with a time step of 0.2 fs. The system's temperature was kept constant using the Berendsen algorithm.[54] The periodic box, with a box length of 18.17 Å, contained one $HCOO^-$ and 199 water molecules, corresponding to the experimental density of pure water. Long-range interactions were treated using the reaction-field procedure.[55] In the present study, the HF/MM and B3LYP/MM simulations were carried out independently with system re-equilibration for 30000 time steps, followed by another 450000 (HF/MM) and 250000 (B3LYP/MM) time steps to collect configurations every tenth step.

3. Results and Discussion

3.1. Structural Details. The characteristics of hydrogen bonds between $HCOO^-$ and water can be interpreted through the O−O_w and O−H_w RDFs, together with their corresponding integration numbers, as shown in Figure 2a and b, respectively. In this context, the first atom in the RDFs refers to the atom of $HCOO^-$, and the latter, with the subscript "w", represents the atom of water molecules. Because the behavior of hydrogen bonds in pure solvent represents a most important reference, the corresponding atom−atom RDFs for pure water obtained at a similar QM/MM level of accuracy[56] were utilized for comparison, as shown in Figure 3. In the HF/MM simulation, the first O−O_w peak is located at 2.76 Å, where integration up to the corresponding first O−O_w minimum yields an average coordination number of 3.45. In the B3LYP/MM simulation, the first O−O_w peak is found at the shorter distance of 2.67 Å, with a lower coordination number of 2.90. The second peaks in the O−O_w RDFs are broad and less pronounced, and they correspond to the contributions of both bulk waters and water molecules in the first hydration layer of the other $HCOO^-$ oxygen.

In accordance with the O−O_w RDFs, the HF/MM and B3LYP/MM simulations reveal first O−H_w peaks, an indicative of $HCOO^-$−water hydrogen bonds, with maxima at 1.84 and 1.71 Å, respectively. Integrations up to the corresponding first

TABLE 2: Optimized Parameters of the Analytical Pair Potentials for the Interaction of Water with $HCOO^-$[a]

pair	A	B	C	D
	HF-Based Method			
	kcal mol^{-1} $Å^4$	kcal mol^{-1} $Å^8$	kcal mol^{-1}	$Å^{-1}$
$C-O_w$	5.161390×10^5	-3.019987×10^4	-7.559447×10^5	1.955784
$O-O_w$	-2.665243×10^5	-5.276995×10^6	6.778200×10^7	3.556668
$H-O_w$	3.248683×10^5	-4.992158×10^5	-1.720448×10^5	1.318893
$C-H_w$	-2.368418×10^5	4.358412×10^5	7.864110×10^5	2.016779
$O-H_w$	5.356162×10^4	1.264105×10^4	-5.753688×10^5	3.105469
$H-H_w$	-3.889529×10^4	6.586156×10^3	1.236351×10^6	3.485256
	B3LYP-Based Method			
	kcal mol^{-1} $Å^4$	kcal mol^{-1} $Å^5$	kcal mol^{-1}	$Å^{-1}$
$C-O_w$	4.136774×10^5	-2.883495×10^5	-1.557409×10^4	0.429679
$O-O_w$	1.336006×10^6	-5.599642×10^6	5.529706×10^7	3.128274
$H-O_w$	9.683479×10^5	-9.298010×10^5	-3.549124×10^5	1.323072
$C-H_w$	2.720650×10^3	5.285593×10^4	2.761879×10^4	1.427650
$O-H_w$	-1.358645×10^5	1.516713×10^5	9.597746×10^4	1.431782
$H-H_w$	-8.338373×10^4	4.962553×10^4	7.038974×10^5	2.987790

[a] Interaction energies in kcal·mol^{-1} and distances in Å.

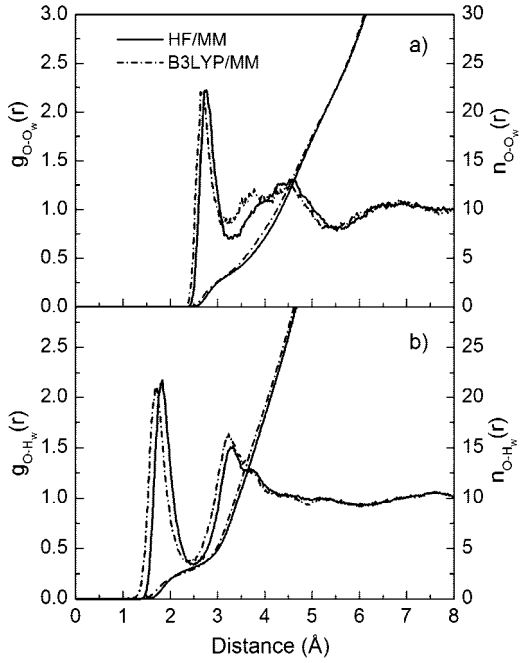

Figure 2. (a) $O-O_w$ and (b) $O-H_w$ radial distribution functions and their corresponding integration numbers.

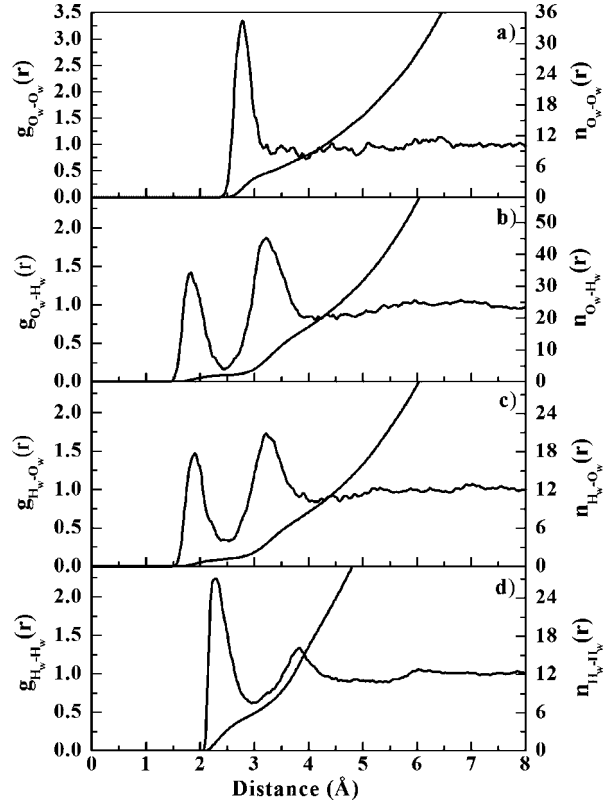

Figure 3. (a) O_w-O_w, (b) O_w-H_w, (c) H_w-O_w, and (d) H_w-H_w radial distribution functions and their corresponding integration numbers. The first atom of each pair refers to the atoms of the water molecule, whose oxygen position was defined as the center of the QM region during the QM/MM simulation.

$O-H_w$ minima give the average values of 3.14 and 2.71, respectively. With respect to both HF/MM and B3LYP/MM simulations, the observed numbers of water oxygen and hydrogen atoms suggest that the first-shell waters are linearly hydrogen bonded to each of the $HCOO^-$ oxygens, that is, they are acting as hydrogen-bond donors. In comparison to the first peak of pure water O_w-H_w RDFs (cf. Figure 3), for example, in terms of shape and peak height, it is obvious that the $O\cdots H_w-O_w$ hydrogen bond interactions are relatively stronger. In the HF/MM and B3LYP/MM simulations, the closest $O\cdots H_w$ distances are 1.38 and 1.17 Å, respectively, compared to the shortest $O_w\cdots H_w$ distance of 1.45 Å for bulk water. The second peak in the $O-H_w$ RDFs near 3.2 Å can be assigned to the hydrogen atoms of first-shell waters that are not hydrogen-bonded to the $HCOO^-$ oxygens.

According to both HF/MM and B3LYP/MM simulations, each $HCOO^-$ oxygen atom is predicted to form more hydrogen bonds with surrounding water molecules than the experimental value of about 2.5.[37,38] In fact, as the first minimum peaks of $O-O_w$ and $O-H_w$ RDFs are rather broad, the number of first-shell waters is quite sensitive to the defined $O-O_w$ and $O-H_w$ minima. For example, integrations up to $O-O_w$ distance of about 0.2 Å shorter than the corresponding $O-O_w$ minima yield 2.53 and 2.47 water oxygens for the HF/MM and B3LYP/MM simulations, respectively. Thus, the differences between our data and experiment are well within the methodical limits of integration on the one hand and interpretation of experimental data on the other. The recent CPMD study,[40] although providing

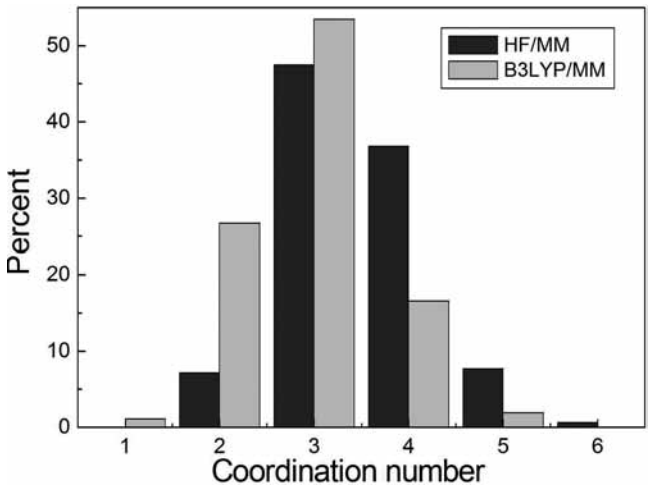

Figure 4. Distributions of the number of water's oxygen atoms at each of $HCOO^-$ oxygens, calculated within the first minimum of the $O-O_w$ RDFs.

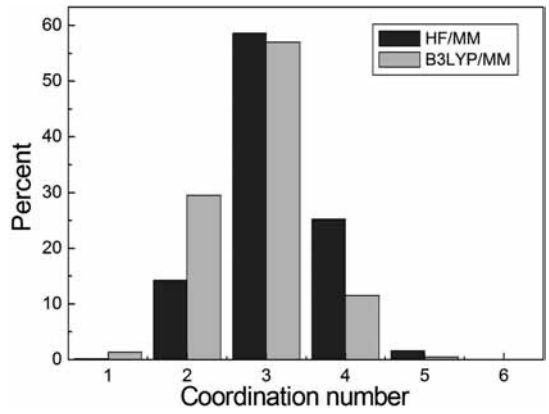

Figure 5. Distributions of the number of water's hydrogen atoms at each of $HCOO^-$ oxygens, calculated within the first minimum of the $O-H_w$ RDFs.

a coordination number apparently identical with experiment, delivers deviating results when a different simulation cell size as well as different functionals (i.e., BLYP and PW91) are employed in the simulations. For example, the use of the BLYP functional had predicted a hydration number of 2.45 per $HCOO^-$ oxygen, while the PW91 method gave a large variation in the hydration numbers ranging from 2.12 to 2.66. Possible weaknesses of the density functional methods could be attributed to the incompleteness of the kinetic energy term, the self-interaction error, and the more or less empirical parametrization, which did not contain any hydrogen-bonded system.

The distributions of oxygen and hydrogen atoms of first-shell waters, calculated with respect to the first minimum of the $O-O_w$ and $O-H_w$ RDFs, are depicted in Figures 4 and 5, respectively. In the HF/MM simulation, the most frequent hydration number per $HCOO^-$ oxygen atom is 3, followed by 4, 2, and 5 in decreasing amounts. In the B3LYP/MM simulation, a prevalent value of 3 is also observed, followed by 2 and 4 in smaller amounts. Figures 6 and 7 show examples of time dependence of the hydration number at each of $HCOO^-$ oxygens within the first 10 ps of the HF/MM and B3LYP/MM simulations, respectively. In both HF/MM and B3LYP/MM trajectories, it is found that the two $HCOO^-$ oxygen atoms simultaneously form asymmetric solvation shells, that is, each of them hydrogen bonding to different numbers of water molecules. Consequently, this causes numerous possible species

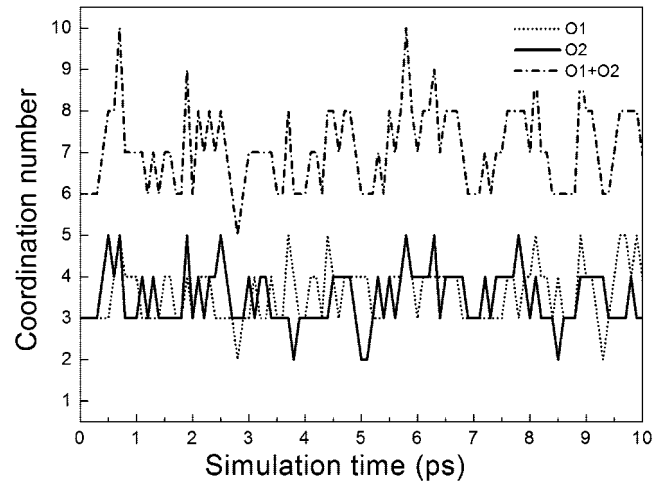

Figure 6. Time dependence of the number of first-shell waters at $HCOO^-$ oxygen atoms, selecting only for first 10 ps of the HF/MM simulation.

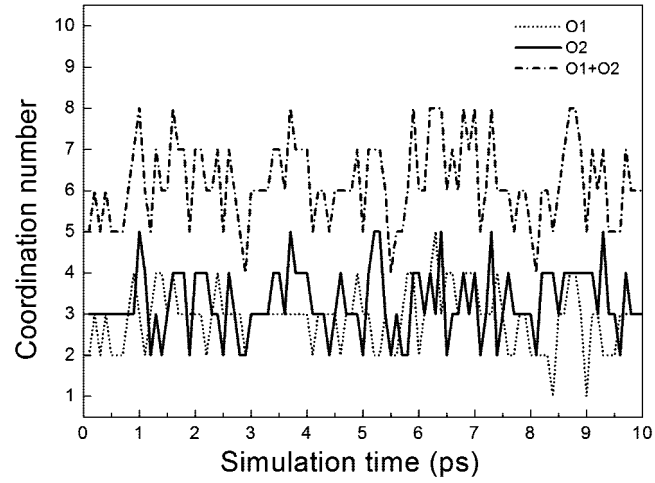

Figure 7. Time dependence of the number of first-shell waters at $HCOO^-$ oxygen atoms, selecting only for first 10 ps of the B3LYP/MM simulation.

of the $HCOO^-$−water complexes to coexist in aqueous solution. As can be seen in Figures 6 and 7, the total numbers of water molecules in the vicinity of $HCOO^-$ oxygens show large fluctuations, ranging from 5 to 10 and from 4 to 8 for the HF/MM and B3LYP/MM simulations, respectively.

A more detailed interpretation of the $HCOO^-$−water hydrogen bonds can be deduced from the probability distributions of the $C-O\cdots H_w$ and $O\cdots O_w-H_w$ angles, calculated within the first minimum of the $O-O_w$ RDFs, as shown in Figures 8 and 9, respectively. In the case that solvent effects would cause strong charge localization on $HCOO^-$, an asymmetrical charge distribution at the two $HCOO^-$ oxygens, corresponding to a formation of a C−O single and a C═O double bond, could exist in aqueous solution. With regard to this point, one could expect the arrangement of directional $C-O\cdots H_w$ hydrogen bonds that cause the $C-O\cdots H_w$ angle to peak at 109.5° and 120°, depending on the type of involved oxygen. In both HF/MM and B3LYP/MM simulations, the observed broad $C-O\cdots H_w$ angular distributions (Figure 8) clearly suggest the absence of such phenomenon. In addition, with regard to the Mulliken charge analyses of several $HCOO^-$−water complexes, there is no substantial charge concentration at one of the $HCOO^-$ oxygens. Apparently, $HCOO^-$ adopts an electronically delocalized structure in aqueous solution, which may fluctuate due

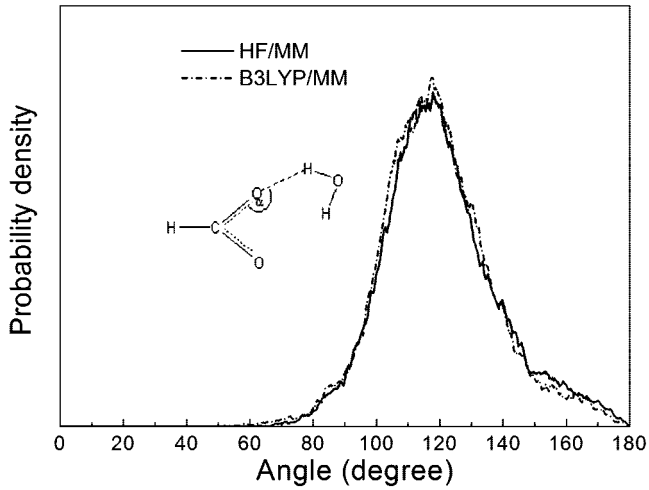

Figure 8. Distributions of C−O---H_w angle, calculated within first minimum of the O−O_w RDFs.

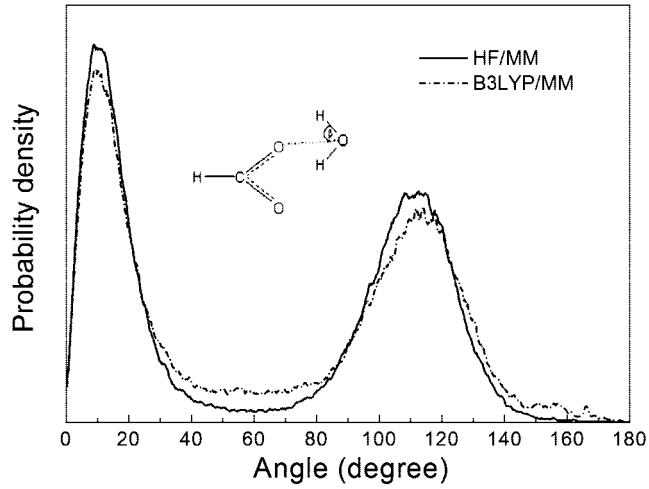

Figure 9. Distributions of O---O_w−H_w angle, calculated within first minimum of the O−O_w RDFs.

to solvent exchange processes. Figure 9 shows the distributions of O···O_w−H_w angle, which clarify the preference for linear O···H_w−O_w arrangements.

3.2. Dynamical Details. In this section, the dynamical data regarding the intramolecular geometry of $HCOO^-$ and the exchange processes of water molecules at $HCOO^-$ oxygens are reported. The geometrical arrangement of $HCOO^-$ in aqueous solution is explained in terms of the distributions of C−O and C−H bond lengths as well as of H−C−O and O−C−O angles, as shown in Figures 10 and 11, respectively. In addition, the distribution of the angle ϕ, as defined by a vector along the C−H bond and a vector pointing outward between the other two C−O bonds, is also given in Figure 12. As compared to the gas phase $HCOO^-$ structure, both HF/MM and B3LYP/MM simulations clearly indicate a substantial change in the local structure of $HCOO^-$ according to the influence of water environment, in particular, a C−O bond lengthening, shortening of the C−H bond and a decrease of the O−C−O angle.

According to Figure 2, the nonzero first minimum of the O−O_w and O−H_w RDFs obtained by both HF/MM and B3LYP/MM simulations clearly suggests an easy exchange of water molecules between the solvation shell and the bulk. The exchange processes of first-shell waters at each of the $HCOO^-$ oxygen atoms can be visualized through the plots of the O−O_w distances against the simulation time, as shown in Figures 13 and 14 for the HF/MM and B3LYP/MM simulations, respectively. During the first 10 ps of the HF/MM and B3LYP/MM trajectories, numerous water molecules can be interchanged between the first shell and the bulk, leading to large fluctuations in the hydration number at each of the $HCOO^-$ oxygen atoms (e.g., see inserts in Figures 13 and 14). Inside the hydration shell, water molecules are either loosely or tightly bound to

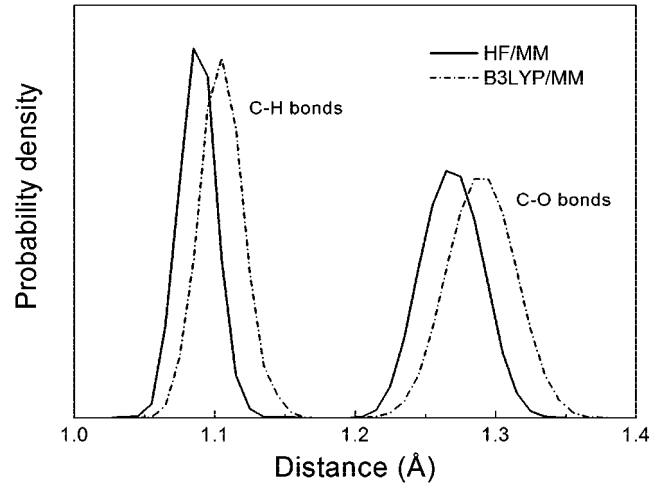

Figure 10. Distributions of C−H and C−O bond lengths.

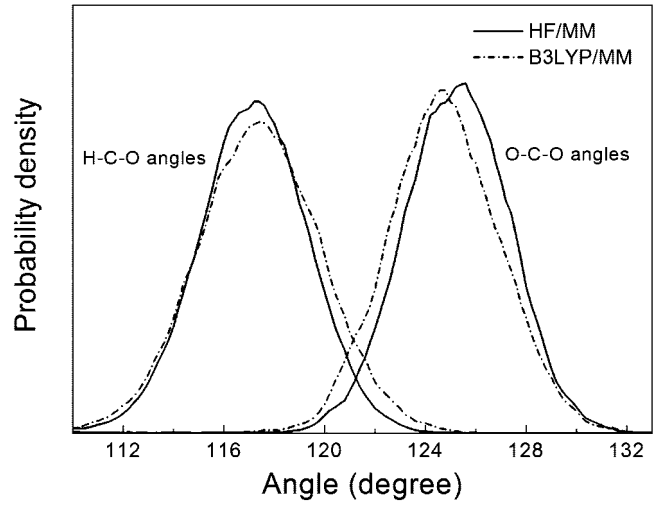

Figure 11. Distributions of H−C−O and O−C−O angles.

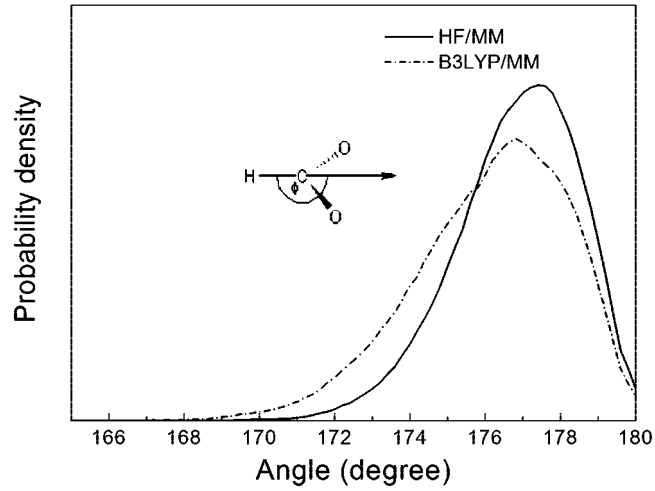

Figure 12. Distributions of ϕ, as defined by a vector along the C−H bond and a vector pointing outward between the two C−O bonds.

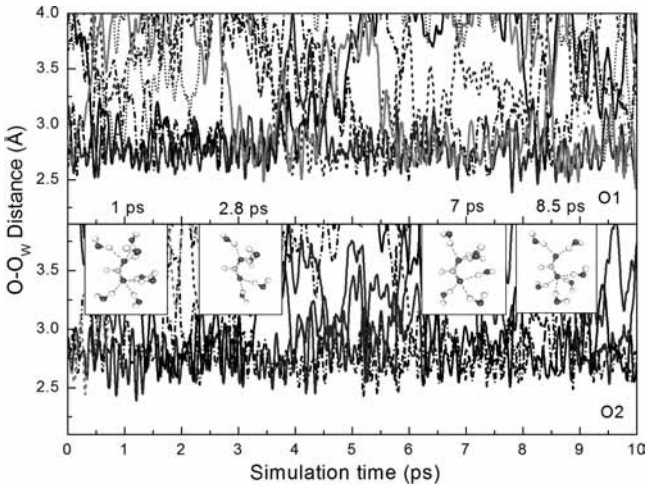

Figure 13. Time dependence of O---O_w distances, selecting only for first 10 ps of the HF/MM trajectories.

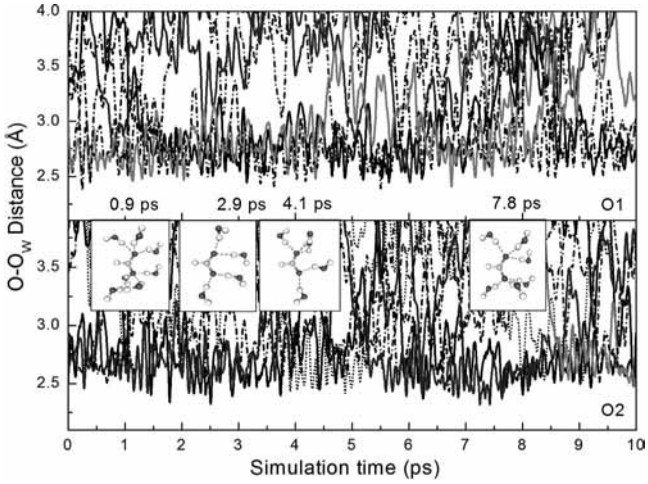

Figure 14. Time dependence of O---O_w distances, selecting only for first 10 ps of the B3LYP/MM trajectories.

$HCOO^-$ oxygen, that is, some first-shell waters temporarily form a hydrogen bond with $HCOO^-$ oxygen, then leaving or even entering again, while others form longer hydrogen bonds to the respective $HCOO^-$ oxygen. On the basis of both HF/MM and B3LYP/MM simulations, the occurrence of bifurcated hydrogen bonds (cf. Figure 1a) appears rare in aqueous solution. First-shell water molecules also preferentially associate with one $HCOO^-$ oxygen atom or the other, rather than adopting simultaneous coordination to both.

The rate of water exchange processes at each $HCOO^-$ oxygen atom was evaluated through mean residence times (MRT) of the surrounding water molecules. In this work, the MRT data were calculated using the direct method,[57] as the product of the average number of nearest-neighbor water molecules located within the first minimum of the O−O_w RDFs with the duration of the simulation, divided by the number of exchange events. With respect to time parameters t^* (i.e., the minimum duration of a ligand's displacement from its original coordination shell to be accounted) of 0.0 and 0.5 ps, the calculated MRT values are summarized in Table 3. In general, the MRT data obtained using $t^* = 0.0$ ps are used for an estimation of hydrogen bond lifetimes, whereas the data obtained with $t^* = 0.5$ ps are considered as a good estimate for sustainable ligand exchange processes.[57] In the HF/MM simulation, the calculated MRT values with respect to $t^* = 0.0$ and 0.5 ps are slightly larger than that of pure water.[56] These data correspond to the observed stronger hydrogen bonds between $HCOO^-$ oxygens and their first-shell water molecules. In the B3LYP/MM simulation, as compared to the B3LYP/MM data for pure water,[46] a clear opposite order of $\tau_{H_2O}(O_i) < \tau_{H_2O}(H_2O)$ is observed. Here it should be noted that the B3LYP/MM results for pure water have produced too slow exchange rates compared to the experimental values.[58] This failure of the B3LYP method to predict the dynamical properties of pure water could be considered as an example for the inadequacy of the DFT methods to correctly describe the characteristics of any aqueous hydrogen-bonded systems. Slow dynamics of aqueous $HCOO^-$, in particular, the $HCOO^-$ rotation, were also observed in the recent CPMD study when the PW91 functional was employed.[40]

TABLE 3: Mean Residence Times of Water Molecules in the Bulk and in the Vicinity of $HCOO^-$ Oxygens[a]

			$t^* = 0.0$ ps		$t^* = 0.5$ ps	
atom/solute	CN	t_{sim}	$N_{ex}^{0.0}$	$\tau_{H_2O}^{0.0}$	$N_{ex}^{0.5}$	$\tau_{H_2O}^{0.5}$
			HF/MM MD			
O1	3.45	70.0	970	0.25	132	1.83
O2	3.44	70.0	1042	0.23	112	2.15
pure H_2O[56]	4.6	12.0	292	0.2	31	1.8
pure H_2O[46]	4.2	40.0		0.33		1.51
			B3LYP/MM MD			
O1	2.84	50.0	810	0.17	57	2.49
O2	2.97	50.0	799	0.19	63	2.36
pure H_2O[46]	4.2	30.0		1.07		7.84

[a] Calculated within the first minimum of the O−O_w RDFs.

4. Conclusion

The QM/MM simulations presented here have produced a detailed picture of $HCOO^-$-water hydrogen bonds in dilute aqueous solution. Both HF/MM and B3LYP/MM simulations predict relatively strong hydrogen bonds between $HCOO^-$ oxygens and first-shell waters. The geometrical arrangement of $HCOO^-$ in aqueous solution is found to be rather flexible and first-shell water molecules can be either "loosely" or "tightly" bound to each of $HCOO^-$ oxygen atoms, forming an asymmetric solvation structure with a varying number of hydrogen bonds, with the prevalent value of 3. Despite the lack of electron correlations, which leads to slightly too long and weak hydrogen bonds, the ab initio HF method proves more reliable than the B3LYP or other DFT approaches, as the latter completely fails to describe the dynamics of ion hydration. Thus, only an extension of the ab initio QM/MM technique by increasing the QM size, enlarging the basis sets and finally including electron correlations would allow a future improvement of the results.

Acknowledgment. This work was supported by the Thailand Research Fund (TRF), under the Royal Golden Jubilee Ph.D. Program (Contract Number PHD/0211/2547). A.T. acknowledges support by the Synchrotron Light Research Institute (SLRI) and Suranaree University of Technology (SUT). B.M.R. acknowledges support by the Austrian Science Foundation (FWF).

References and Notes

(1) Frank, H. *Chemical Physics of Ionic Solutions*; John Wiley & Sons: New York, 1956.
(2) Williams, R. J. P. *Bio-inorganic Chemistry*; American Chemical Society: Washington, DC, 1971.
(3) Cowan, J. A. *Chem. Rev.* **1998**, *98*, 1067.
(4) Ohtaki, H.; Radnai, T. *Chem. Rev.* **1993**, *93*, 1157.

(5) Dang, L. X.; Schenter, G. K.; Glezakou, V. A.; Fulton, J. L. *J. Phys. Chem. B* **2006**, *110*, 23644.
(6) Angelo, P. D.; Pavel, N. V. *J. Synchrotron Radiat.* **2001**, *8*, 173.
(7) Hewish, N. A.; Neilson, G. W.; Enderby, J. E. *Nature* **1982**, *297*, 138.
(8) Howell, I.; Neilson, G. W. *J. Phys.: Condens. Matter* **1996**, *8*, 4455.
(9) Impey, R. W.; Madden, P. A.; McDonald, I. R. *J. Phys. Chem.* **1983**, *87*, 5071.
(10) Bopp, P. *The Physics and Chemistry of Aqueous Ionic Solutions*; Reidel Publishing Company: Boston, MA, 1987; p 217.
(11) Heinzinger, K. *Pure Appl. Chem.* **1985**, *57*, 1031.
(12) Lee, S. H.; Rasaiah, J. C. *J. Phys. Chem.* **1996**, *100*, 1420.
(13) Obst, S.; Bradaczek, H. *J. Phys. Chem.* **1996**, *100*, 15677.
(14) Ebner, C.; Sansone, R.; Hengrasmee, S.; Probst, M. *Int. J. Quantum Chem.* **1999**, *75*, 805.
(15) Stone, J. A. *The Theory of Intermolecular Forces*; Clarendon Press: Oxford, 1996.
(16) Elrod, M. J.; Saykally, R. J. *Chem. Rev.* **1994**, *94*, 1975.
(17) Rode, B. M.; Schwenk, C. F.; Tongraar, A. *J. Mol. Liq.* **2004**, *110*, 105.
(18) Car, R.; Parrinello, M. *Phys. Rev. Lett.* **1985**, *55*, 2471.
(19) Marx, D.; Hutter, J. In *Modern Methods and Algorithms of Quantum Chemistry*; Grotendorst, J., Ed.; NIC: FZ Jülich, 2000.
(20) Chen, B.; Ivanov, I.; Park, J. M.; Parrinello, M.; Klein, M. L. *J. Phys. Chem.* **2000**, *106*, 12006.
(21) Tuckerman, M. E.; Marx, D.; Klein, M. L.; Parrinello, M. *Science* **1997**, *275*, 817.
(22) Brugé, F.; Bernasconi, M.; Parrinello, M. *J. Am. Chem. Soc.* **1999**, *121*, 10883.
(23) Tuckerman, M. E.; Marx, D.; Parrinello, M. *Nature* **2002**, *417*, 925.
(24) Warshel, A.; Levitt, M. *J. Mol. Biol.* **1976**, *103*, 227.
(25) Singh, U. C.; Kollman, P. A. *J. Comput. Chem.* **1986**, *7*, 718.
(26) Field, M. J.; Bash, P. A.; Karplus, M. *J. Comput. Chem.* **1990**, *11*, 700.
(27) Gao, J. *Rev. Comput. Chem.* **1996**, *7*, 119.
(28) Kerdcharoen, T.; Liedl, K. R.; Rode, B. M. *Chem. Phys.* **1996**, *211*, 313.
(29) Tongraar, A.; Liedl, K. R.; Rode, B. M. *J. Phys. Chem. A* **1998**, *102*, 10340.
(30) Tongraar, A.; Rode, B. M. *Phys. Chem. Chem. Phys.* **2003**, *5*, 357.
(31) Tongraar, A.; Rode, B. M. *Chem. Phys. Lett.* **2005**, *403*, 314.
(32) Tongraar, A.; Rode, B. M. *Chem. Phys. Lett.* **2005**, *409*, 304.
(33) Intharathep, P.; Tongraar, A.; Sagarik, K. *J. Comput. Chem.* **2005**, *26*, 1329.
(34) Rode, B. M.; Schwenk, C. F.; Hofer, T. S.; Randolf, B. R. *Coord. Chem. Rev.* **2005**, *249*, 2993.
(35) Tongraar, A.; Tangkawanwanit, P.; Rode, B. M. *J. Phys. Chem. A* **2006**, *110*, 12918.
(36) Kuntz, I. D. *J. Am. Chem. Soc.* **1971**, *93*, 514.
(37) Kameda, Y.; Mori, T.; Nishiyama, T.; Usuki, T.; Uemura, O. *Bull. Chem. Soc. Jpn.* **1996**, *69*, 1495.
(38) Kameda, Y.; Fukuhara, K.; Mochiduki, K.; Naganuma, H.; Usuki, T.; Uemura, O. *J. Non-Cryst. Solids* **2002**, *312*−*314*, 433.
(39) Jorgensen, W. L.; Gao, J. *J. Phys. Chem.* **1986**, *90*, 2174.
(40) Leung, K.; Rempe, S. B. *J. Am. Chem. Soc.* **2004**, *126*, 344.
(41) Brooks, B. R.; Bruccoleri, R. E.; Olafson, B. D.; States, D. J.; Swaminathan, S.; Karplus, M. *J. Comput. Chem.* **1983**, *4*, 187.
(42) Dunning, T. H. Jr.; Hay, P. J. *Modern Theoretical Chemistry, III*; Plenum: New York, 1976.
(43) Dunning, T. H. *J. Chem. Phys.* **1989**, *90*, 1007.
(44) Kendall, R. A.; Dunning, T. H.; Harrison, R. J. *J. Chem. Phys.* **1992**, *96*, 6769.
(45) Woon, D. E.; Dunning, T. H. *J. Chem. Phys.* **1993**, *98*, 1358.
(46) Xenides, D.; Randolf, B. R.; Rode, B. M. *J. Chem. Phys.* **2005**, *122*, 174506.
(47) Tongraar, A.; Kerdcharoen, T.; Hannongbua, S. *J. Phys. Chem. A* **2006**, *110*, 4924.
(48) Stillinger, F. H.; Rahman, A. *J. Chem. Phys.* **1976**, *68*, 666.
(49) Bopp, P.; Jancsó, G.; Heinzinger, K. *Chem. Phys. Lett.* **1983**, *98*, 129.
(50) Frisch, M. J.; Trucks, G. W.; Schlegel, H. B.; Scuseria, G. E.; Robb, M. A.; Cheeseman, J. R.; Zakrewski, V. G.; Montgomery, J. A.; Stratmann, R. E.; Burant, J. C.; Dapprich, S.; Millam, J. M.; Daniels, A. D.; Kudin, K. N.; Strain, M. C.; Farkas, O.; Tomasi, J.; Barone, V.; Cossi, M.; Cammi, R.; Mennucci, B.; Pomelli, C.; Adamo, C.; Clifford, S.; Ochterski, J.; Peterson, G. A.; Ayala, P. Y.; Cui, Q.; Morokuma, K.; Malick, D. K.; Rabuck, A. D.; Raghavachari, K.; Foresman, J. B.; Cioslowski, J.; Ortiz, J. V.; Stefanov, B. B.; Liu, G.; Liashenko, A.; Piskorz, P.; Komaromi, I.; Gomperts, R.; Martin, R. L.; Fox, D. J.; Keith, T.; Al-Laham, M. A.; Peng, C. Y.; Nanayakkara, A.; Gonzalez, C.; Challacombe, M.; Gill, P. M. W.; Johnson, B. G.; Chen, W.; Wong, M. W.; Andres, J. L.; Head-Gordon, M.; Replogle, E. S.; Pople, J. A. *Gaussian 98*; Gaussian, Inc.: Pittsburgh, PA, 1998.
(51) Carpenter, J. E.; Weinhold, F. *J. Mol. Struct.: THEOCHEM* **1988**, *169*, 41.
(52) Reed, A. E.; Weinstock, R. B.; Weinhold, F. *J. Chem. Phys.* **1985**, *83*, 735.
(53) Reed, A. E.; Curtiss, L. A.; Weinhold, F. *Chem. Rev.* **1988**, *88*, 899.
(54) Berendsen, H. J. C.; Postma, J. P. M.; van Gunsteren, W. F.; DiNola, A.; Haak, J. R. *J. Phys. Chem.* **1984**, *81*, 3684.
(55) Adams, D. J.; Adams, E. H.; Hills, G. J. *Mol. Phys.* **1979**, *38*, 387.
(56) Tongraar, A.; Rode, B. M. *Chem. Phys. Lett.* **2004**, *385*, 378.
(57) Hofer, T. S.; Tran, H. T.; Schwenk, C. F.; Rode, B. M. *J. Comput. Chem.* **2004**, *25*, 211.
(58) Lock, A. J.; Woutersen, S.; Bakker, H. J. *Femtochemistry and Femtobiology*; World Scientific: Singapore, 2001.

JP810341U